:UMENTATION PAGE

Form Approved
OMB No. 0704-0188

1. AGENCY USE ONLY (Leave blank)	2. REPORT DATE	3. REPORT TYPE AND DATES COVERED

4. TITLE AND SUBTITLE

Distribution of Trapped Electrons at Interface States in ACTFEL Devices

5. FUNDING NUMBERS

DAAL03-91-G-0242

6. AUTHOR(S)

S. Kobayashi, J.F. Wager, A. Abu-Dayah

7. PERFORMING ORGANIZATION NAME(S) AND ADDRESS(ES)

Oregon State University
Department of Electrical and Computer Engineering
Corvallis, OR 97331-3211

8. PERFORMING ORGANIZATION REPORT NUMBER

9. SPONSORING/MONITORING AGENCY NAME(S) AND ADDRESS(ES)

U. S. Army Research Office
P. O. Box 12211
Research Triangle Park, NC 27709-2211

10. SPONSORING/MONITORING AGENCY REPORT NUMBER

ARO 28852.2-PH

11. SUPPLEMENTARY NOTES

The view, opinions and/or findings contained in this report are those of the author(s) and should not be construed as an official Department of the Army position, policy, or decision, unless so designated by other documentation.

12a. DISTRIBUTION/AVAILABILITY STATEMENT

Approved for public release; distribution unlimited.

12b. DISTRIBUTION CODE

13. ABSTRACT *(Maximum 200 words)*

The distribution of trapped electrons at interface states in alternating-current thin-film electroluminescent (ACTFEL) devices is assessed using a new field-stimulated charge measurement technique in which the polarization charge transient is measured experimentally and curve fit using a model for the dynamic emission of electrons from interface states. The trapped electron distribution is relatively small at low energy but rises abruptly at approximately 0.6-0.8 eV below the conduction band minimum for an ACTFEL device with SiON insulators.

By	
Distribution/	
Availability Codes	
Dist	Avail and/or Special
A-1	

14. SUBJECT TERMS

ACTFEL, Electroluminescence, Interface States, Electrical Characterization, ZnS:Mn

15. NUMBER OF PAGES

16. PRICE CODE

17. SECURITY CLASSIFICATION OF REPORT	18. SECURITY CLASSIFICATION OF THIS PAGE	19. SECURITY CLASSIFICATION OF ABSTRACT	20. LIMITATION OF ABSTRACT
UNCLASSIFIED	UNCLASSIFIED	UNCLASSIFIED	UL

DISTRIBUTION OF TRAPPED ELECTRONS AT INTERFACE STATES IN ACTFEL DEVICES

S. Kobayashi,† J.F. Wager, and A. Abu-Dayah, Department of Electrical and Computer Engineering, Center for Advanced Materials Research, Oregon State University, Corvallis, OR 97331-3211
†Permanent address: Nippon Sheet Glass Co., Ltd., Tsukuba, Japan

ABSTRACT

The distribution of trapped electrons at interface states in alternating-current thin-film electroluminescent (ACTFEL) devices is assessed using a new field-stimulated charge measurement technique in which the polarization charge transient is measured experimentally and curve fit using a model for the dynamic emission of electrons from interface states. The trapped electron distribution is relatively small at low energy but rises abruptly at approximately 0.6-0.8 eV below the conduction band minimum for an ACTFEL device with SiON insulators.

1. INTRODUCTION

Interface states are known to play a critical role in the operation of alternating-current thin-film electroluminescent (ACTFEL) devices. In spite of the importance of interface states in establishing the electron emission and trapping characteristics required for ACTFEL operation, very little is known about the energy depth or density at which electrons are trapped at the interface. An interface trap energy of 0.8 eV[1-3] or 1.8 eV[4] has been estimated experimentally by thermally stimulated current (TSC) measurements. Theoretical estimates of the interface trap energy, based on the assumption that electrons tunnel from interface states, yield values in the range of 0.6 to 1.0 eV.[5-6]

In this paper, we present a new field-stimulated charge measurement technique and estimate the distribution of trapped electrons at interface states. It is important to note that we assess the trapped electron density at interface traps, which we denote N_{te}, which is not identical to the interface state density, N_{ss}, even though both of these quantities are expressed in units of eV^{-1} cm^{-2}. N_{ss} is a thermodynamic quantity which must be evaluated under quasi-equilibrium conditions (in practice N_{ss} is normally evaluated at steady-state) whereas N_{te} is assessed under non-steady-state conditions.

2. EXPERIMENTAL TECHNIQUE

A. Measurement Set Up

The devices measured herein are conventional ACTFEL devices consisting of an ITO electrode, an evaporated ZnS:Mn phosphor layer, sputtered SiON insulators, and an Al electrode. The device area is 0.079 cm^2. The ACTFEL devices are aged for 12 hours at a frequency of 1 kHz and a maximum applied bias of 220 V to ensure good device stability.

A Sawyer-Tower circuit is used for the measurement, as shown in Fig. 1. The applied voltage waveform employed is indicated in Fig. 2 with energy band diagrams corresponding to various conditions under which the ACTFEL device operates.

Each half period of the applied waveform is comprised of three distinct pulses. The "filling pulse" is a 20 μs voltage pulse used to fill the interface states with electrons. Immediately following the filling pulse is a "measuring pulse" of 40 μs duration whose amplitude is varied to control the internal field in the ZnS from approximately 0 to 1.4 MV/cm. The energy band diagrams shown in Fig. 2 corresponding V_1, V_2, and V_n illustrate how the measuring pulse amplitude can be used to set the internal phosphor field. Notice also that the magnitude of the measuring pulse amplitude can be used to probe interface states of different energy depths. The external voltage, $V_{ex}(t)$, and Sawyer-Tower sense capacitor voltage, $V_{cs}(t)$, transients are monitored using a Tektronix model 7854 digitizing oscilloscope during the measuring pulse duration. Finally, the "rest pulse," in which the external voltage is zero, comprises the remaining portion of the applied voltage half cycle. The measurements are performed in a dark environment to avoid external photon excitation. All of the reported data are for the ITO interface.

B. Theory

The field-stimulated charge measurement consists of measuring $V_{ex}(t)$ and $V_{cs}(t)$ at various measuring pulse amplitudes. The internal polarization charge stored at the interface, $Q_{pol}(t)$, and the electric field in the ZnS, F(t), are obtained from

$$Q_{pol}(t) = \frac{C_i + C_p}{C_i} C_s V_{cs}(t) - C_p V_{ex}(t) \quad (1)$$

$$F(t) = \frac{C_s}{C_i d_p} V_{cs}(t) - \frac{1}{d_p} V_{ex}(t) \quad (2)$$

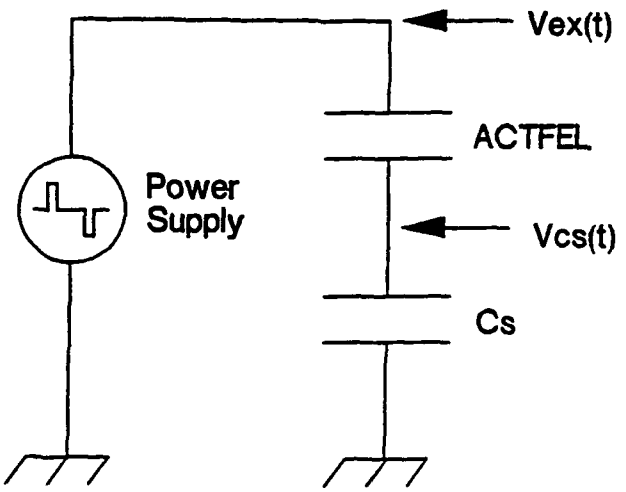

Figure 1. Circuit used for ACTFEL characterization.

where C_i is the total insulator capacitance, C_p is the ZnS phosphor capacitance, C_s is the capacitance of the sense capacitor, and d_p is the ZnS phosphor thickness.

The basic qualitative idea underlying the field-stimulated charge technique is as follows. After the filling pulse fills interface states with electrons, the measuring pulse sets the internal phosphor field to a given value. Electrons are thus emitted from interface states due to the application of the measuring pulse. The energy depth from which the interface electrons are emitted depends on the magnitude of the measuring pulse amplitude. $Q_{pol}(t)$ as obtained from (1) is a reflection of interface charge; a decrease in Q_{pol} corresponds to a reduction of the interface charge. Assessment of the density of trapped electrons at interface states, N_{te}, is accomplished by fitting a portion of the transient $Q_{pol}(t)$ curve using a dynamic model as described below.

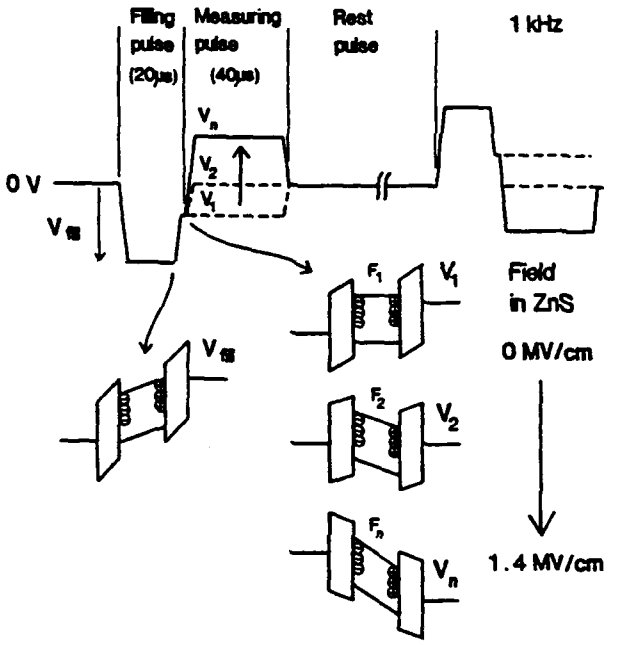

Figure 2. Driving voltage waveform and corresponding energy band diagrams.

Note that the internal phosphor field, F(t), is not constant during the measuring pulse duration since electrons emitted from interface states and transported across the phosphor provide a negative feedback effect which reduces F.[6] In order to make a quantitative estimate of N_{te}, we consider only a portion of the $Q_{pol}(t)$ curve in which the field varies by less than 5%. Since F(t) is approximately constant over the relevant portion of $Q_{pol}(t)$, we assume that this portion of the decay transient arises from the emission of electrons from a discrete interface level with the interface state emission kinetics described by

$$\frac{dN_e(t)}{dt} = -e_n N_e(t) \quad (3)$$

where $dN_e(t) = dQ_{pol}(t)/q$ and where $N_e(t)$ is the total number of electrons trapped at interface states in units of number of states per square centimeter and e_n is the emission rate of electrons from the discrete interface state.

We assume that e_n is comprised of three possible emission mechanisms: (a) thermal emission with Poole-Frenkel barrier lowering, $e_n(PF)$; (b) pure tunneling $e_n(PT)$; and (c) phonon-assisted tunneling, $e_n(PAT)$; such that the total emission rate is given by

$$e_n = e_n(PF) + e_n(PT) + e_n(PAT) . \tag{4}$$

Figure 3 illustrates the three emission modes from a discrete interface level and also indicates Poole-Frenkel barrier lowering as ΔE_i while E_i is the interface trap depth with respect to the conduction band minimum. Quantitatively, these emission mechanisms are calculated via the following expressions.[7,8]

$$e_n(PF) = \sigma v_{th} N_c \exp\left[-\frac{E_i - \Delta E_i}{k_B T}\right] \tag{5}$$

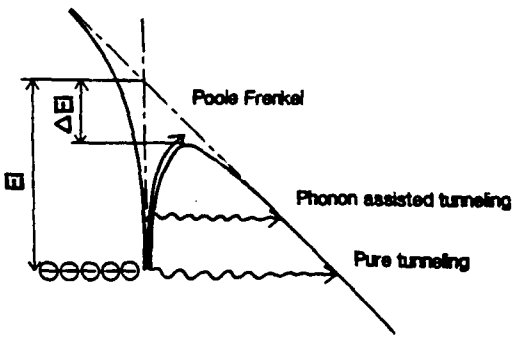

Figure 3. Three modes of electron emission from a discrete trap state.

where

$$\Delta E_i = q\left[\frac{qF}{\pi\epsilon}\right]^{1/2} , \tag{6}$$

$$e_n(PT) = \frac{qF}{4\left(2m^* E_i\right)^{1/2}} \exp\left[\left[-\frac{8\pi}{3}\frac{\left(2m^*\right)^{1/2} E_i^{3/2}}{qhF}\right]\left[1-\left[\frac{\Delta E_i}{E_i}\right]^{5/3}\right]\right] , \tag{7}$$

$$e_n(PAT) = \sigma V_{th} N_c \exp\left[-\frac{E_i}{k_B T}\right] \int \exp\left[z - z^{3/2}\left[\frac{8\pi}{3}\frac{\left(2m^*\right)^{1/2}(k_B T)^{3/2}}{qhF}\right]\left[1-\left[\frac{\Delta E_i}{z k_B T}\right]^{5/3}\right]\right] dz , \tag{8}$$

where z is a normalized energy given by

$$z = \frac{E_i}{k_B T} . \tag{9}$$

Note that (5)-(9) correspond to electron emission from a coulombic well whereas if ΔE_i is set equal to zero (5)-(9) correspond to emission from a Dirac well; both cases are considered in our subsequent analysis. Also note that σ, the interface trap capture cross-section, is the only unknown parameter in (5)-(9). We find that above 1 MV/cm e_n is dominated by pure tunneling so that the magnitude of σ is not critical in our present analysis.

Quantitative estimation of the trapped electron density, N_{te}, is accomplished as follows. A portion of the $Q_{pol}(t)$ transient is curve fit using (3)-(9) in order to achieve optimal agreement between the experimental data and the simulated curve. Two fitting parameters, E_i and $N_e(0)$ [i.e., N_e at t = 0], are adjusted in the curve fit optimization. Thus, if $Q_{pol}(t)$ is measured as a function of the measuring pulse amplitude, a family of values of $N_e(0)$ and E_i may be obtained. A plot of $N_e(0)$ versus E_i (e.g., see Fig. 5) is then generated and a N_{te} plot (e.g., see Fig. 6) may be obtained from

$$N_{te} = \frac{d N_e(0)}{d E_i} . \tag{10}$$

Equation (10) is analogous to the interface state density defining equation.[9]

3. RESULTS AND DISCUSSION

A plot of the measured and curve fit $Q_{pol}(t)$ transients is shown in Fig. 4. Zero time in Fig. 4 corresponds to a 2-3 μs delay after the measuring pulse is applied to avoid possible artifacts caused by switching on the measuring pulse. The duration of the $Q_{pol}(t)$ waveform used in the curve fitting corresponds to 16 μs or to the time at which F(t) decreases to 95% of its initial value, whichever time is smaller. This constraint on the curve fitting duration ensures that F is relatively constant.

A plot of $N_e(0)$ versus E_i is presented in Fig. 5 for filling pulse voltage amplitudes, V_{fill} = 200, 220, and 240 V. As expected, a larger filling voltage results in the filling of more interface states.

Figure 6 illustrates a plot of N_{te} versus E_i for three values of the filling pulse voltage amplitude. These curves may appear surprising if one expects to see an interface state plot since N_{ss} should not change with variations in V_{fill}. However, recall that we are estimating the density of trapped electrons, N_{te}, not N_{ss}. N_{te} can be envisaged as an effective interface state density which is determined by both the interface state density and a nonequilibrium occupancy function which is established by the kinetics of interface state emission as specified by the dynamical equations (3)-(9).

To understand the kinetic aspects of N_{te} more clearly, refer to Fig. 7 which is a plot of e_n versus E_i with F as a parameter. Recall that $Q_{pol}(t)$ is curve fit over a nominal duration beginning at 2 μs and ending at 18 μs which corresponds to measurement emission rates of 5×10^5 s^{-1} and 5.6×10^4 s^{-1} as indicated by the dashed lines shown in Fig. 7. Thus, for the measurement duration used and for the range of phosphor field employed, electrons within a certain range of trap depth are measurable. For example, from Fig. 7 we estimate that for F between 0 to 1.4 MV/cm we can measure interface states with E_i between about 0.35 to 0.9 eV.

Returning to Fig. 6, N_{te} now may be interpreted as the density of filled interface states with emission time constants of 2-18 μs for fields between 0 and 1.4 MV/cm. The trend indicated in Fig. 6 in which the N_{te} signal increases in magnitude with an increase in V_{fill} and shifts to smaller E_i simply arises from the fact that larger values of V_{fill} result in the filling of more interface states and that

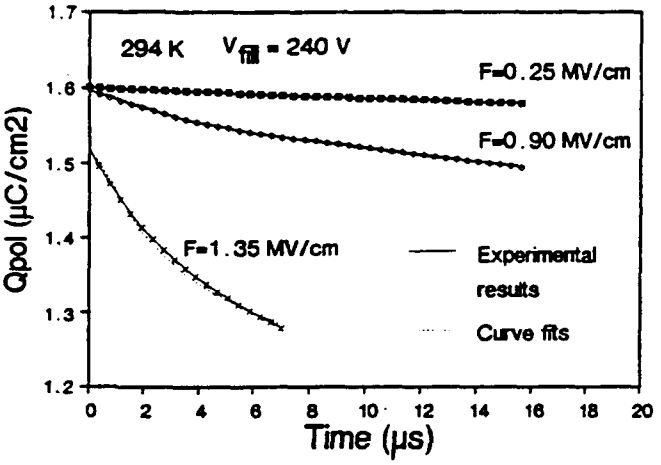

Figure 4. Transient polarization charge at various internal ZnS phosphor fields.

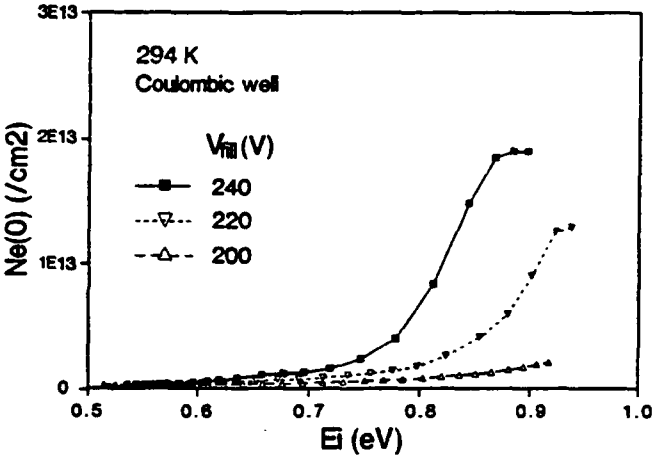

Figure 5. $N_e(0)$ versus E_i at various filling pulse amplitudes.

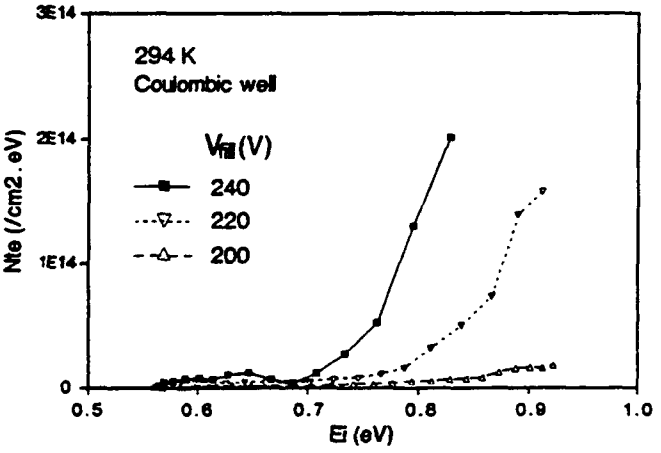

Figure 6. Trapped electron density versus trap energy depth for various filling pulse amplitudes.

those states tend to be located at smaller energies since the deeper states are already filled. These curves suggest that N_{te} is probably relatively small up to approximately 0.7-0.8 eV, above which it rises sharply. Figure 6 indicates that an exceedingly large number of electrons can be accommodated in trapping states at the SiON/ZnS interface. The high energy portion of the curve where N_{te} decreases, which is not plotted in Fig. 6, offers no useful information with regard to the magnitude of N_{te} since this decreasing trend is due to kinetic considerations, as explained by Fig. 7.

Figure 6 is calculated assuming that interface state emission is best modeled as arising from a coulombic barrier. A comparison is made in Fig. 8 for N_{te} assuming either a coulombic or Dirac well. Note that if a Dirac well is assumed, the N_{te} curve moves to lower energy by about 0.1 eV. The rise in N_{te} is then estimated as occurring at approximately 0.6-0.7 eV if a Dirac well is used. It is not clear whether emission from interface states in an ACTFEL device is best modeled by a coulombic or Dirac well.

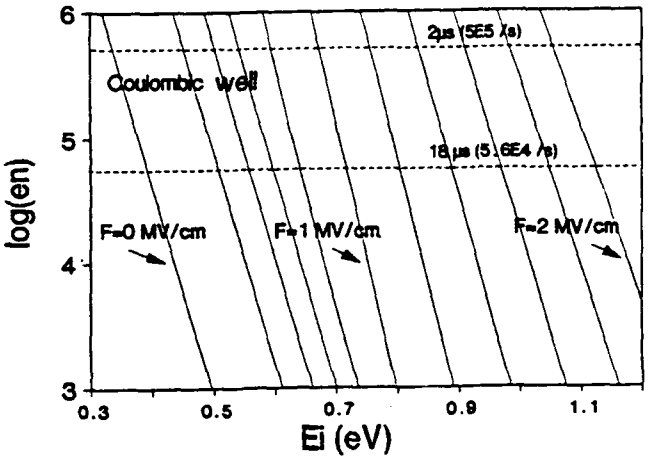

Figure 7. Emission rate from a coulombic well discrete trap versus trap energy depth as a function of internal ZnS phosphor field.

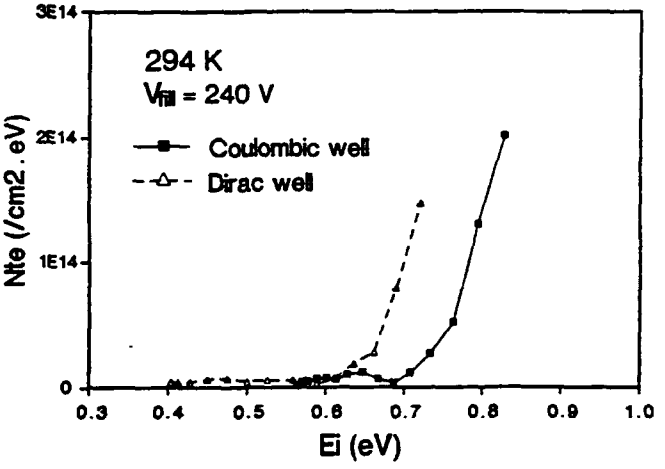

Figure 8. Trapped electron density versus trap energy depth for coulombic and Dirac wells.

4. CONCLUSIONS

A new field-stimulated charge measurement technique is employed in order to estimate the density of trapped electrons at interface states in an ACTFEL device. The trapped electron density depends both on the interface density and on the dynamics of interface state emission. We estimate the trapped electron density to be relatively small, up to about 0.6-0.8 eV, above which it abruptly increases.

5. ACKNOWLEDGMENTS

We wish to thank Ron Khormaei and Chris King of Planar Systems, Inc. for providing samples and helpful suggestions. The work was supported by the U.S. Army Research Office under contract D11L03-91G0242.

REFERENCES

1. T. Inoguchi and S. Mito, *Electroluminescence*, edited by J.I. Pankove, *Topics in Applied Physics*, Vol. 17 (Springer, Heidelberg), 197 (1977).
2. K. Miyashita and M. Shibata, *Digest of Japan Display*, 100 (1983).
3. T. Shibata, et al., Extended Abstracts (The 34th Spring Meeting); *The Japan Soc. of Appl. Phys. and Related Societies*, No. 3, 879 (1987) (in Japanese).
4. Y. Sano and K. Nunomura, *Electroluminescence*, edited by S. Shionoya and H. Kobayashi, *Springer Proceedings in Physics*, Vol. 38, (Springer, Heidelberg), 77 (1977).
5. D.H. Smith, *J. Lumin. 23*, 209 (1981).
6. E. Bringuier, *J. Appl. Phys. 66*, 1314 (1989).

7. G. Vincent, A. Chantre, and D. Bois, *J. Appl. Phys. 50*, 5484 (1979).
8. E. Rosencher, V. Mosser, and G. Vincent, *Phys. Review 29*, 1135 (1983).
9. S.M. Sze, *Physics of Semiconductor Devices*, 2nd ed. (Wiley, New York), 379 (1981)